JACS Au
AN OPEN ACCESS JOURNAL OF THE AMERICAN CHEMICAL SOCIETY

pubs.acs.org/jacsau

Article

Elucidation of Electrochemically Induced but Chemically Driven Pt Dissolution

Junsic Cho, Haesol Kim,* Hyung-Suk Oh, and Chang Hyuck Choi*

Cite This: *JACS Au* 2023, 3, 105−112

Read Online

ACCESS | Metrics & More | Article Recommendations | Supporting Information

ABSTRACT: Securing the electrochemical durability of noble metal platinum is of central importance for the successful implementation of a proton exchange membrane fuel cell (PEMFC). Pt dissolution, a major cause of PEMFC degradation, is known to be a potential-dependent transient process, but its underlying mechanism is puzzling. Herein, we elucidate a chemical Pt dissolution process that can occur in various electrocatalytic conditions. This process intensively occurs during potential perturbations with a millisecond timescale, which has yet to be seriously considered. The open circuit potential profiles identify the dominant formation of metastable Pt species at such short timescales and their simultaneous dissolution. Considering on these findings, a proof-of-concept strategy for alleviating chemical Pt dissolution is further studied by tuning electric double layer charging. These results suggest that stable Pt electrocatalysis can be achieved if rational synthetic or systematic strategies are further developed.

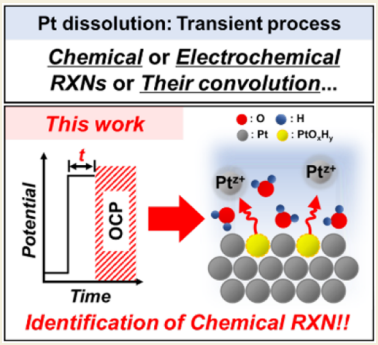

KEYWORDS: *corrosion, fuel cells, heterogeneous catalysis, operando analysis, platinum*

INTRODUCTION

Proton exchange membrane fuel cells (PEMFCs) have attracted significant attention for implementation in green and sustainable energy economies because they can generate electricity from clean hydrogen fuels.[1,2] Platinum is a core element of commercialized PEMFCs and exhibits superior activity toward both hydrogen oxidation (HOR) and oxygen reduction reactions (ORRs).[2−5] The initial catalytic performance of Pt electrocatalysts has recently reached a sufficient standard by alloying with other transition metals or modifying nanostructures and supporting substrates.[5−9] Consequently, securing their long-term durability is the next quest for successful PEMFC distribution since Pt electrocatalysts are often exposed to highly corrosive conditions. Especially PEMFC electrodes encounter potential excursions or spikes at highly anodic potentials, especially during fuel starvation and start-up/shut-down (SU/SD) events (up to 2.0 and 1.6 V_{RHE} for fuel starvation and SU/SD, respectively), inducing severe degradation of Pt electrocatalysts (and carbon support) and ultimately deteriorating PEMFC performance.[10,11]

Therefore, a comprehensive understanding of Pt degradation is critical to achieve durable PEMFC operation. Despite significant efforts pioneered by Johnson et al. in 1970,[12] the insufficient resolution and sensitivity of spectroscopic analyses hinder a solid grasp of the detailed Pt degradation mechanism. Recently, great advances in *operando* spectroscopic analyses have enabled more detailed understanding of the degradation mechanisms of Pt electrocatalysts, particularly Pt dissolution.[13−16] For instance, online inductively coupled plasma-mass spectrometry coupled with an electrochemical flow cell (EFC/ICP-MS) successfully detects Pt dissolution during electrochemical operations, unveiling that Pt dissolution is a transient process accompanying substantial changes in the surface chemistry and structure of Pt (Figure 1a and Figure S1).[17−23] Moreover, it has been revealed that Pt dissolution can be influenced by various parameters such as facet, reactant, pH, temperature, etc.[16−18,21,22] Although previous studies have achieved a potential-resolved and quantitative understanding of Pt dissolution, the underlying Pt dissolution mechanisms during the transition process are highly vague.[23−25] For instance, a number of electrochemical and chemical Pt dissolution reactions have been proposed as possible Pt dissolution mechanisms, but their deconvolutions and even verifications of any reaction paths have yet to be clearly accomplished.

Herein, we demonstrate that chemical corrosion occurs on electrochemically induced unstable Pt surfaces. This conclusion is supported by our Pt dissolution study using EFC/ICP-MS under multiple potential pulses with different pulse widths (t). In particular, an electrically disconnected condition immediately after the potential pulses allows the distinction of chemical dissolution from the complex convolution of unknown dissolution pathways during the transient process.

Received: August 29, 2022
Revised: October 23, 2022
Accepted: October 26, 2022
Published: January 12, 2023

https://doi.org/10.1021/jacsau.2c00474
JACS Au 2023, 3, 105−112

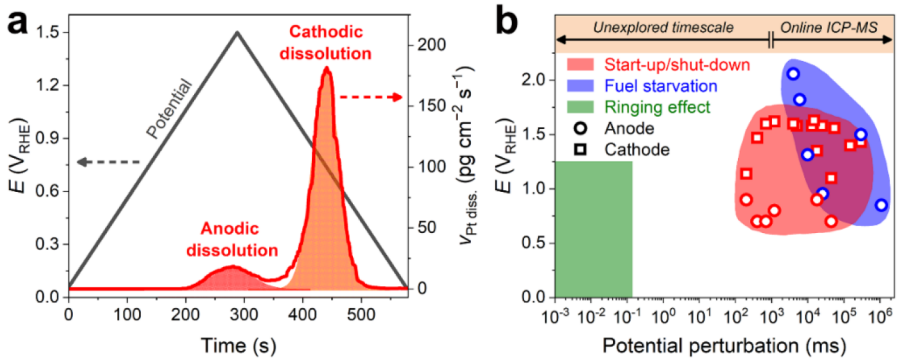

Figure 1. Pt degradation process. (a) Real-time Pt dissolution measured by an online EFC/ICP-MS during a cyclic voltammetry (CV), with a scan rate of 5 mV s^{-1} in a potential range of 0.05−1.5 V_{RHE} in Ar-saturated 0.1 M $HClO_4$ electrolyte. (b) Electrode potentials and potential perturbation durations observed during or used for describing the SU/SD and fuel starvation events in the literature.[26−33] For better identification, each event accelerating the PEMFC degradation is grouped and indicated with a shaded area. Previous Pt dissolution studies using the EFC/ICP-MS cover most conditions of the SU/SD and fuel starvation events, but unexplored conditions still remain, where the ringing effect possibly occurs when the electrical circuit is connected or applied potential is changed.[32,33]

By taking advantage of the open circuit potential (OCP), the formation of metastable Pt and its spontaneous dissolution can be identified as the origin of the chemical Pt dissolution process. We further confirm that chemical Pt dissolution, which has not been seriously considered as one of Pt dissolution pathways because this event occurs in electrochemical environments, is transposable to more practically relevant conditions. Combined with the knowledge of the electric double layer (EDL), we discuss a proof-of-concept strategy for alleviating chemical Pt dissolution during rapid potential disturbance.

RESULTS AND DISCUSSION

Platinum dissolution on a polycrystalline Pt electrode was investigated in Ar-saturated 0.1 M $HClO_4$ using online EFC/ICP-MS (Figure S2), during eight consecutive potential pulses. The potential pulses were set to 1.5 V_{RHE}, and their t was varied from 0.2 ms to 1000 s. After the anodic polarization at 1.5 V_{RHE}, the electrode potential dropped to 0.05 V_{RHE} and held there for 7 min to stabilize the ICP-MS signals. This series of potential excursions is referred to as Protocol 1 (P^1), and each pulse of the protocol is denoted as P^1_t, depending on its t. It is worth noting that this protocol covers most of the potential perturbation durations of the detrimental processes of PEMFC operations, such as fuel starvation and SU/SD events during real PEMFC operations (Figure 1b).[26−33]

In Protocol 1, no distinct Pt dissolution is found at $P^1_{0.2ms}$ (Figure 2a). However, a trace amount of Pt (0.42 pg cm^{-2} s^{-1}) starts to dissolve at P^1_{1ms}, and dissolution becomes intensified from 2.6 to 7.1 pg cm^{-2} s^{-1} as the t increased from 10 ms to 1000 s. This observation indicates that Pt dissolution can be initiated at a very short potential perturbation (i.e., 1 ms), which has not been rigorously addressed so far. For longer t of P^1_{100s} and P^1_{1000s}, clear anodic and cathodic Pt dissolutions are distinguishable at a potential jump to 1.5 V_{RHE} and a sequential potential drop to 0.05 V_{RHE}, respectively. The cathodic dissolution is more pronounced than anodic dissolution, and negligible Pt dissolution is shown during the potential hold at 1.5 V_{RHE} for P^1_{1000s}. This result is consistent with previous reports, verifying that Pt dissolution is a transient process.[14,16] However, the anodic and cathodic Pt dissolutions are hardly distinguishable at t below 10 s, probably due to the insufficient resolution of our EFC/ICP-MS system at a such short t, i.e., signal tailing.

To investigate the Pt dissolution behavior more clearly, we performed an experiment analogous to Protocol 1, referred to as Protocol 2 (P^2). In Protocol 2, after the potential jump and hold at 1.5 V_{RHE} for t, the electrode potential was released to an OCP for 5 min, followed by a potential hold at 0.05 V_{RHE} for 7 min. This additional OCP step was employed to deconvolute the contribution of anodic and cathodic dissolutions and further provided an opportunity to observe possible chemical dissolution processes. It is of note that a potential jump followed by the OCP is a practically feasible event for PEMFCs during SU/SD operations.[27−30]

Interestingly, during Protocol 2, the Pt dissolution rate for each potential pulse increases by approximately 1 order of magnitude at t below 10 s compared to that during Protocol 1 (Figure 2b, c). Pt redeposition and cathodic dissolution hardly govern the enhanced Pt dissolution rate because the dissolution increment in Protocol 2 occurs prior to the potential drop (from OCP to 0.05 V_{RHE}). In addition, since Pt electrode experienced an identical potential excursion at the initial stage of all the potential pulses, i.e., the potential jump from 0.05 to 1.5 V_{RHE} (the potential rising time is shorter than 2 μs, much shorter than t for $P^2_{0.2ms}$), increased anodic dissolution can also be ruled out as the cause of enhanced Pt dissolution during Protocol 2. For instance, for P^2_{100s} and P^2_{1000s}, the anodic dissolution rates are almost identical, i.e., 2.2 ± 0.2 pg cm^{-2} s^{-1}, the values of which are also comparable with those for P^2_{100s} and P^1_{1000s} of Protocol 1 (Figure S3). Surprisingly, the amount of such anodic dissolutions is quantitatively much lower than the Pt dissolution at short durations of potential pulses in Protocol 2, i.e., P^2_t for t = 10 ms−10 s. This cannot be adequately explained by electrochemical Pt dissolution alone, because the charge passed at P^2_{100s} and P^2_{1000s} (and also P^1_{100s} and P^1_{1000s}) is much larger than that at P^2_t for t = 10 ms−10 s. Nevertheless, nonelectrochemically driven chemical Pt dissolution is clearly identified during the OCP step after the potential hold at 1.5 V_{RHE}. Especially, a non-negligible amount of Pt (~1.7 ng cm^{-2}) was dissolved during the OCP step for P^2_{100s}. This Pt dissolution signal is not an artifact induced by the signal tailing of anodic Pt dissolution because anodic dissolution is undoubtedly distinguishable from a subsequent plateau, and is much lower even than that of

https://doi.org/10.1021/jacsau.2c00474
JACS Au 2023, 3, 105−112

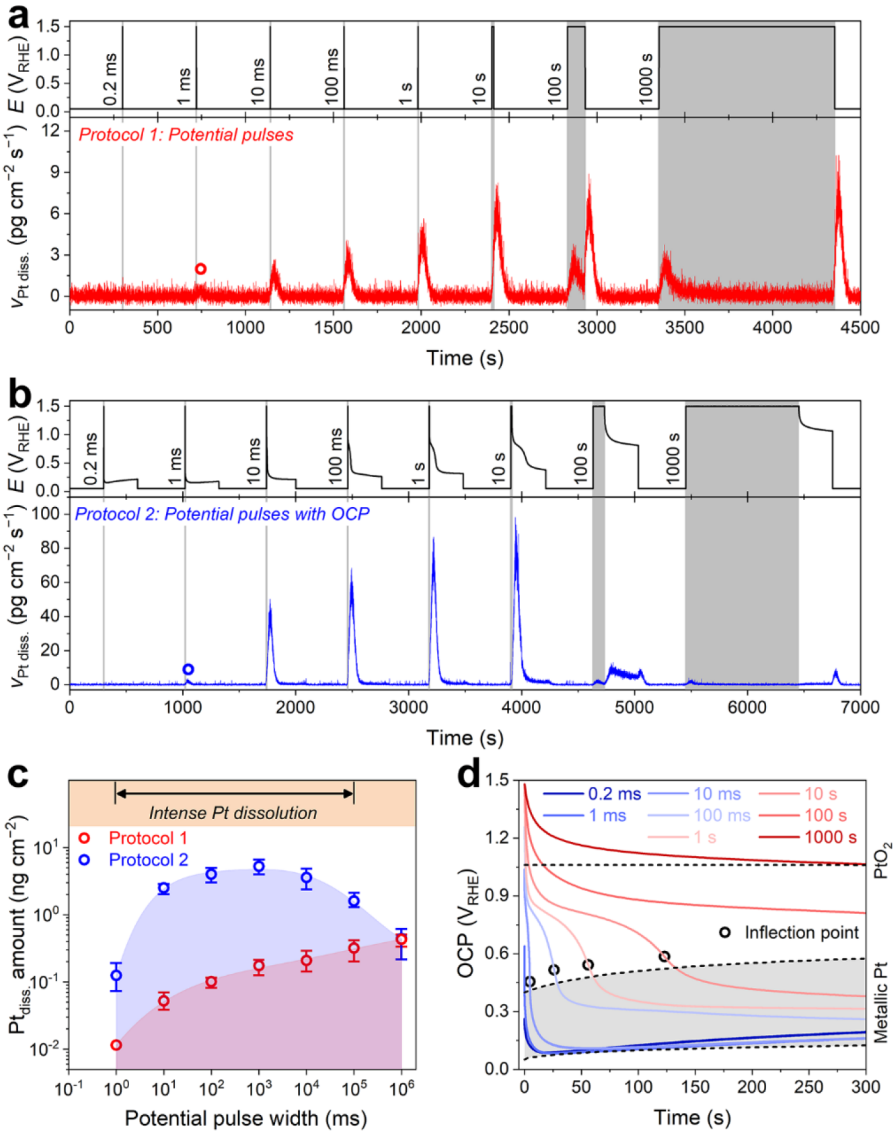

Figure 2. Stability evaluation of the polycrystalline Pt during pulsed potential disturbances. Real-time Pt dissolution measured by an online EFC/ICP-MS during (a) Protocol 1 and (b) Protocol 2 in Ar-saturated 0.1 M $HClO_4$ electrolyte. The pulse width, *t*, increases from 0.2 ms to 1000 s, and the lowest *t*, where the Pt dissolution is discernible, is highlighted with a hollow circle. (c) Dissolved Pt amount at each potential pulse. (d) OCP profiles just after potential pulses of the Protocol 2. Their inflection points are marked with hollow circles. As references, OCP values of PtO_2 and metallic Pt with and without H_{UPD} are also shown by dashed lines.

chemical dissolution (max. ~7 pg cm^{-2} s^{-1}). For P^2_{1000s}, although it is relatively insignificant, the chemical Pt dissolution during OCP step is also discernible (~0.4 pg cm^{-2} s^{-1}), before which Pt dissolution signal converges to almost zero value (baseline) during a 1000 s potential hold at 1.5 V_{RHE}. These findings allow us to conclude that chemical Pt dissolution indeed exists during the electrochemically driven transient process of Pt. Therefore, we can reasonably deduce that the origin of the unexpected larger Pt dissolution in Protocol 2 than in Protocol 1 at a relatively low *t* is attributed to chemical Pt dissolution. An identical conclusion was made from control experiments with an O_2-saturated 0.1 M $HClO_4$, which is a more realistic condition for the PEMFC cathode than the Ar-saturated one (Figures S4 and S5), and with an opposite order of potential pulses from 1000 s to 0.2 ms (Figure S6).

The OCP profiles during Protocol 2 further reveal that the slow kinetics of the stable Pt oxide formation results in different amounts of chemical Pt dissolution depending on *t*. In the literature, partially oxidized Pt species, e.g., PtO_xH_y, have been proposed as the main cause of chemical Pt dissolution (see the Supplementary Note for a detailed discussion).[34−36] Unfortunately, the exact chemical nature of metastable Pt species is not clearly understood (and even defined) owing to their unstable and short-lived characteristics, which are hardly measurable using typical *ex situ* analyses. Alternatively, the formation of metastable species on Pt can be electrochemically deduced from OCP profiles because it reflects the equilibrium potential between the electrode and the electrolyte and is very sensitive to the chemical nature of the electrode surface.[37]

Figure 2d shows considerable OCP changes of the Pt electrode for 300 s after its potential hold at 1.5 V_{RHE} for different *t*. It is of note that, to avoid any interferences from

https://doi.org/10.1021/jacsau.2c00474
JACS Au 2023, 3, 105−112

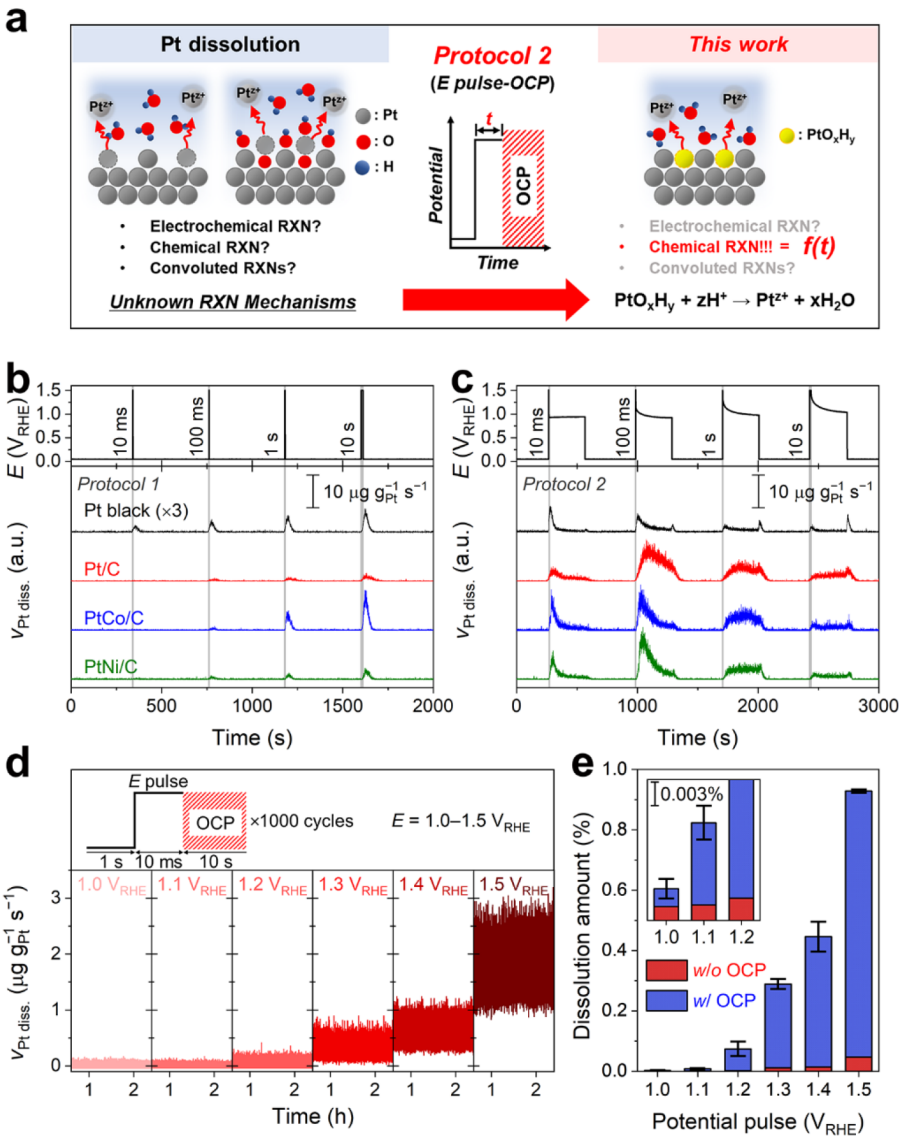

Figure 3. Verification of the broad applicability of the chemical Pt dissolution in more realistic conditions. (a) Summary of this work identifying chemical Pt dissolution from unclear and complex Pt dissolution processes. Real-time Pt dissolution of Pt black, Pt/C, PtCo/C, and PtNi/C measured by an online EFC/ICP-MS during (b) Protocol 1 and (c) Protocol 2 (see Figures S9–12 for the data of all t of 0.2 ms–1000 s). (d) Real-time Pt dissolution of Pt black during 1000 potential pulses (t = 10 ms, E = 1–1.5 V_{RHE}). For clear comparisons, a part of online EFC/ICP-MS signals was collected and shown at each potential. (e) Accumulated amounts of Pt dissolved during the 1000 potential pulses with and without the OCP steps.

redox-active O_2 and H_2 molecules, in this measurement the electrochemical cell and electrolyte were continuously purged with Ar, and the counter electrode was physically separated from the Pt working electrode using a Nafion membrane (Figure S2). This result is in contrast to the case of the potential perturbation-free metallic Pt and fully oxidized PtO_2, which show OCP values of 0.12–0.58 V_{RHE} (depending on the absence and presence of hydrogen underpotential deposition, H_{UPD}) and ~1.1 V_{RHE}, respectively (Figure S7). For P^2_{1000s}, at which insignificant chemical Pt dissolution is observed (Figure S3), its OCP value is stabilized at ~1.1 V_{RHE}, indicating formation of a stable outer PtO_2. On the other hand, for P^2_t(t = 10 ms–10 s), the OCPs are quickly stabilized and reached a potential range of 0.7–0.9 V_{RHE} within a few tens of seconds. Since these quasi-stabilized OCP values are located between those of metallic Pt and PtO_2, the result implies the formation of partially oxidized Pt on the surface (i.e., PtO_xH_y) after the potential hold at 1.5 V_{RHE} for 10 ms–10 s. Afterward, their OCP values converge to ~0.3 V_{RHE}, which is positioned between OCP values of H_{UPD} and its free Pt surfaces. In addition, as t increases, the quasi-stabilized OCP values are anodically shifted, and their windows (defined here as the time at the inflection point of the OCP curves) become elongated. Hence, the results reveal that the inner metallic Pt is gradually exposed to the electrolyte through the continuous chemical dissolution of the outer PtO_xH_y species, the amount of which is magnified as the potential perturbation time, t, increases. We note that the chemical Pt dissolution is a dominant process under open circuit conditions since the OCP profile does not originate from the self-discharge of the polarized Pt via the Faradaic reactions (Figure S8).[38−40] Nevertheless, for P^2_t(t < 10 ms), their OCP values quickly rebounded to ~0.1 V_{RHE},

https://doi.org/10.1021/jacsau.2c00474
JACS Au 2023, 3, 105–112

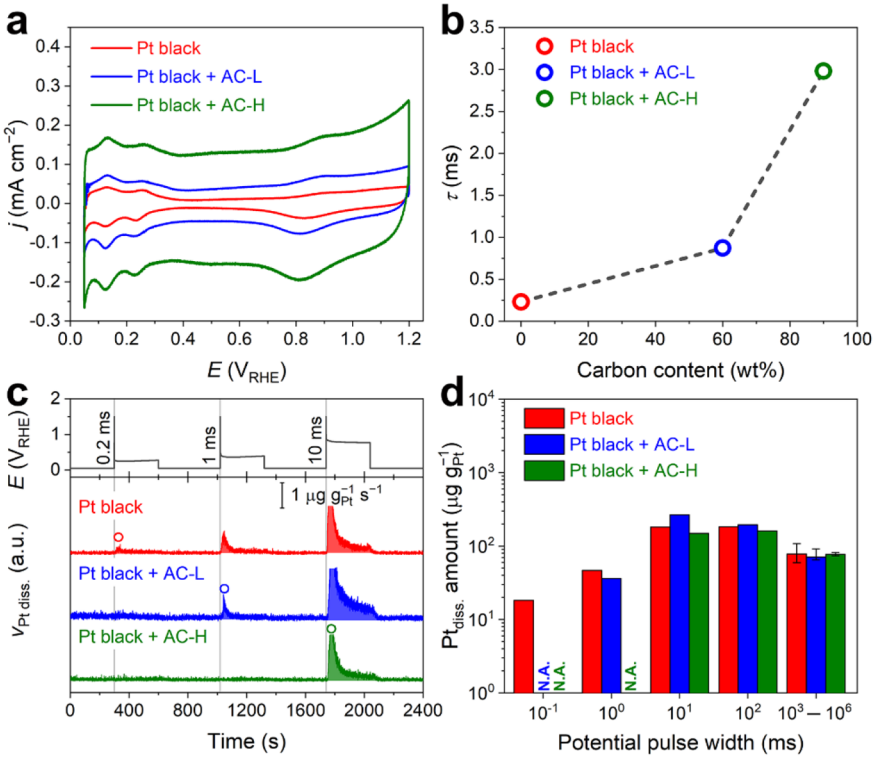

Figure 4. Proof-of-concept strategy for mitigating the chemical Pt dissolution. (a) CVs and (b) calculated τ of the Pt black electrodes with different AC amounts in Ar-saturated 0.1 M $HClO_4$ electrolyte. (c) Real-time Pt dissolution signals of the Pt black electrodes monitored by online EFC/ICP-MS during Protocol 2 (see Figure S16 for the data at t > 10 ms). The lowest t where the Pt dissolution is discernible is highlighted with a hollow circle. (d) Dissolved Pt amount at each potential pulse for the Pt black electrodes.

probably due to insufficient time duration for desorbing all the H_{UPD} generated during chronoamperometry (CA) at 0.05 V_{RHE} prior to the potential perturbation.

To summarize our findings, the OCP step after the short duration of potential pulses enables the deconvolution of chemical Pt dissolution from the unclear and complex Pt dissolution process during electrochemical Pt transitions (Figure 3a), and the duration of the potential perturbation, t, is identified as a key parameter governing the extent of chemical Pt dissolution. For t less than 100 s, the chemical Pt dissolution is intensified as the t becomes longer owing to the increased formation of metastable PtO_xH_y. However, for t longer than 100 s, PtO_xH_y further transforms to stable Pt oxides, leading to a considerable suppression of chemical Pt dissolution. This turning point, predicted here by the decline of the chemical Pt dissolution, is well matched with previous results reported by Imai et al., who showed a partially oxidized Pt is fully converted to PtO_2 after 100 s polarization at 1.4 V_{RHE} through *in situ* X-ray absorption spectroscopy (XAS).[36]

We then studied the chemical Pt dissolution process under various electrochemical conditions to understand whether this event is only limited to the polycrystalline Pt electrode at the potential pulse of 1.5 V_{RHE}. Pt dissolution rates were measured with Pt black nanoparticles during Protocols 1 and 2 (Figure 3b, c and Figure S9). Similar to the polycrystalline Pt, the results show much magnified Pt dissolution at t = 0.2 ms−10 s in Protocol 2 (rather than that in Protocol 1) and discernible Pt dissolution during OCP steps. For PEMFC-relevant catalysts (i.e., Pt/C, PtCo/C, and PtNi/C), such Pt dissolution behaviors were also found in Protocol 2 (Figure 3b, c and Figures S10−12), inferring that the chemical Pt dissolution also occurs for the conventional Pt-based catalysts as well as the polycrystalline Pt.

Online EFC/ICP-MS study of Pt black nanoparticles, analyzed during repeated 1000 potential pulses with t = 10 ms, further reveals that the chemical Pt dissolution could occur at much moderated potential pulses of 1−1.4 V_{RHE}. With an OCP step immediately after each potential pulse (analogous to Protocol 2), considerably magnified Pt dissolution rates were recorded at all potential pulses of 1−1.5 V_{RHE} compared to those without the OCP step (analogous to Protocol 1; Figure 3d, e). However, the dissolution rate is lowered as the potential decreases (Figures S13 and 14). These control experiments with various materials and potential conditions indicate that the chemical Pt dissolution would be a ubiquitous event, possibly occurring at a potential higher than 1 V_{RHE} for conventional Pt-based catalysts.

The time constant (τ) is a key physical parameter describing the electrode−electrolyte interface properties, which basically represents the characteristic time required to charge a capacitor (C_{dl}) connected to a resistor (R) in series.[41] Once the potential changes, the non-Faradaic current first dominates the overall current flow for charging EDL, and afterward by the Faradaic process (Figure S15). We surmised that this well-known phenomenon might offer an opportunity to prevent undesirable chemical Pt dissolution by delaying the formation of metastable Pt species, if EDL charging process becomes a major event during potential perturbations with short durations. To confirm this hypothesis, we prepared a Pt black electrode, and its τ was sequentially tuned by mixing it with different amounts of the activated carbon (AC). The Pt black electrodes with low and high amounts of AC were

https://doi.org/10.1021/jacsau.2c00474
JACS Au 2023, 3, 105−112

denoted as "Pt black + AC-L" (mass ratio = 4:6) and "Pt black + AC-H" (1:9), respectively. It is of note that increasing R can also increase τ but this is not beneficial for efficient PEMFC operations.

Their CV profiles show an almost identical H_{UPD} response with a similar electrochemical surface area (ECSA) value of 12.5 ± 1 m^2 g_{Pt}^{-1} (Figure 4a), implying no chemical modifications of the Pt black after the physical mixing with AC. Nevertheless, a clear increase in the double layer capacitance is found in the presence of AC on the electrode. The estimated τ values for Pt black, Pt black + AC-L, and Pt black + AC-H are 0.2, 0.9, and 3 ms, respectively (Figure 4b), suggesting that their Faradaic processes can be postponed to the millisecond timescale. The effect of τ on the chemical Pt dissolution was then investigated during Protocol 2 (Figure 4c and Figure S16). AC-free Pt black reveals discernible Pt dissolution at $P^2_{0.2ms}$. However, this signal disappears for Pt black + AC-L, and more interestingly, Pt black + AC-H confirms negligible Pt dissolution even at P^2_{1ms}. The suppressed chemical Pt dissolution is not an artifact induced either by a decrease in the active Pt surface area, or by the increased diffusion path for Pt ions after the introduction of AC, as confirmed by the almost untouched H_{UPD} values and Pt dissolution rates at each potential pulse with t longer than 10 ms (much longer than τ) for all samples (Figure 4a, d). Therefore, we identify a preceded non-Faradaic charging to be a critical process governing the extent of followed metastable Pt formation and consequent its dissolution.

OUTLOOK AND CONCLUSIONS

We demonstrated the presence of chemical Pt dissolution process during its electrochemical excursion, which can become dominant under certain conditions that accompany a short duration of potential perturbations. The OCP profiles identified relatively slow Pt oxidation kinetics, which led to the formation of metastable Pt species, an origin of chemical Pt dissolution, at such a rapid potential perturbation. Along with the above understanding, our additional studies further unveiled the markedly accelerated chemical Pt dissolution even at t of 1000 s in the presence of methanol in acidic medium (Figure S17), and that chemical Pt dissolution can also be arisen in alkaline conditions (Figure S18). These findings highlight that chemical Pt dissolution does not occur in a limited manner under PEMFC conditions, but is likely to be a ubiquitous path of Pt degradation in various electrochemical devices, implying the need for further investigation under various experimental conditions reflecting a wide range of electrochemical energy conversion systems for durable electrocatalysis.

In addition, although we exemplified that mitigation of the chemical Pt dissolution is achievable by introducing AC to tune the EDL parameter τ, this strategy is not suitable for immediate implementation in PEMFCs. This limitation primarily originates from thickened catalyst layer, which strongly affects both the performance and durability of PEMFCs. As already well-understood by several previous experimental and theoretical reports,[3,4,42−44] the thickened catalyst layer not only governs Ohmic loss and mass transportation but also water flooding and even uniformity of potential distribution in PEMFCs. In addition, at relevant timescales of PEMFC operation, a practically nonfeasible amount of AC may be needed to prevent the chemical Pt dissolution (Figure S19). However, this proof-of-concept strategy will provide a fundamental principle for developing future rational strategies, for instance, tuning the internal or external PEMFC components (e.g., additional potential load) to buffer the unavoidable potential perturbations and to minimize the undesirable chemical Pt dissolution.

ASSOCIATED CONTENT

Supporting Information

The Supporting Information is available free of charge at https://pubs.acs.org/doi/10.1021/jacsau.2c00474.

Experimental details; possible generation of the partially oxidized Pt species; CV result of Pt; schematic images of EFC connected to the ICP-MS; real-time Pt dissolution results of Pt black and Pt-based catalysts; OCP profiles of PtO_2 and metallic Pt; modeling of Faradaic and non-Faradaic current responses of a simplified Randles circuit model (PDF)

AUTHOR INFORMATION

Corresponding Authors

Haesol Kim − *Department of Chemistry, Pohang University of Science and Technology (POSTECH), Pohang 37673, Republic of Korea*; Email: hskim0218@postech.ac.kr

Chang Hyuck Choi − *Department of Chemistry, Pohang University of Science and Technology (POSTECH), Pohang 37673, Republic of Korea*; orcid.org/0000-0002-2231-6116; Email: chchoi@postech.ac.kr

Authors

Junsic Cho − *Department of Chemistry, Pohang University of Science and Technology (POSTECH), Pohang 37673, Republic of Korea*

Hyung-Suk Oh − *Clean Energy Research Center, Korea Institute of Science and Technology (KIST), Seoul 02792, Republic of Korea*; orcid.org/0000-0002-0310-6666

Complete contact information is available at: https://pubs.acs.org/10.1021/jacsau.2c00474

Author Contributions

CRediT: **Junsic Cho** formal analysis, investigation, methodology, writing-original draft, writing-review & editing; **Haesol Kim** conceptualization, formal analysis, investigation, project administration, writing-original draft, writing-review & editing; **Hyung-Suk Oh** methodology, resources; **Chang Hyuck Choi** conceptualization, project administration, resources, supervision, writing-original draft, writing-review & editing.

Notes

The authors declare no competing financial interest.

ACKNOWLEDGMENTS

This work was supported by the National Research Foundation of Korea (NRF) grant funded by the Korea government (MSIT) (2019M3D1A1079309 and 2021R1A5A1030054) and by the KIST Institutional Program.

REFERENCES

(1) Eberle, U.; Müller, B.; von Helmolt, R. Fuel Cell Electric Vehicles and Hydrogen Infrastructure: Status 2012. *Energy Environ. Sci.* **2012**, *5* (10), 8780−8798.

(2) Debe, M. K. Electrocatalyst Approaches and Challenges for Automotive Fuel Cells. *Nature* **2012**, *486* (7401), 43−51.

(3) Fan, J.; Chen, M.; Zhao, Z.; Zhang, Z.; Ye, S.; Xu, S.; Wang, H.; Li, H. Bridging the Gap between Highly Active Oxygen Reduction Reaction Catalysts and Effective Catalyst Layers for Proton Exchange Membrane Fuel Cells. *Nat. Energy* **2021**, *6* (5), 475−486.
(4) Chong, L.; Wen, J.; Kubal, J.; Sen, F. G.; Zou, J.; Greeley, J.; Chan, M.; Barkholtz, H.; Ding, W.; Liu, D.-J. Ultralow-Loading Platinum-Cobalt Fuel Cell Catalysts Derived from Imidazolate Frameworks. *Science* **2018**, *362* (6420), 1276−1281.
(5) Kodama, K.; Nagai, T.; Kuwaki, A.; Jinnouchi, R.; Morimoto, Y. Challenges in Applying Highly Active Pt-Based Nanostructured Catalysts for Oxygen Reduction Reactions to Fuel Cell Vehicles. *Nat. Nanotechnol.* **2021**, *16* (2), 140−147.
(6) Chattot, R.; Le Bacq, O.; Beermann, V.; Kühl, S.; Herranz, J.; Henning, S.; Kühn, L.; Asset, T.; Guétaz, L.; Renou, G.; Drnec, J.; Bordet, P.; Pasturel, A.; Eychmüller, A.; Schmidt, T. J.; Strasser, P.; Dubau, L.; Maillard, F. Surface Distortion as a Unifying Concept and Descriptor in Oxygen Reduction Reaction Electrocatalysis. *Nat. Mater.* **2018**, *17* (9), 827−833.
(7) Cui, C.; Gan, L.; Heggen, M.; Rudi, S.; Strasser, P. Compositional Segregation in Shaped Pt Alloy Nanoparticles and their Structural Behaviour during Electrocatalysis. *Nat. Mater.* **2013**, *12* (8), 765−771.
(8) Chen, C.; Kang, Y.; Huo, Z.; Zhu, Z.; Huang, W.; Xin, H. L.; Snyder, J. D.; Li, D.; Herron, J. A.; Mavrikakis, M.; Chi, M.; More, K. L.; Li, Y.; Markovic, N. M.; Somorjai, G. A.; Yang, P.; Stamenkovic, V. R. Highly Crystalline Multimetallic Nanoframes with Three-Dimensional Electrocatalytic Surfaces. *Science* **2014**, *343* (6177), 1339−1343.
(9) Huang, X.; Zhao, Z.; Cao, L.; Chen, Y.; Zhu, E.; Lin, Z.; Li, M.; Yan, A.; Zettl, A.; Wang, Y. M.; Duan, X.; Mueller, T.; Huang, Y. High-Performance Transition Metal−Doped Pt_3Ni Octahedra for Oxygen Reduction Reaction. *Science* **2015**, *348* (6240), 1230−1234.
(10) Jung, S.-M.; Yun, S.-W.; Kim, J.-H.; You, S.-H.; Park, J.; Lee, S.; Chang, S. H.; Chae, S. C.; Joo, S. H.; Jung, Y.; Lee, J.; Son, J.; Snyder, J.; Stamenkovic, V.; Markovic, N. M.; Kim, Y.-T. Selective Electrocatalysis Imparted by Metal−Insulator Transition for Durability Enhancement of Automotive Fuel Cells. *Nat. Catal.* **2020**, *3* (8), 639−648.
(11) Kaspar, R. B.; Wittkopf, J. A.; Woodroof, M. D.; Armstrong, M. J.; Yan, Y. Reverse-Current Decay in Hydroxide Exchange Membrane Fuel Cells. *J. Electrochem. Soc.* **2016**, *163* (5), F377−F383.
(12) Johnson, D. C.; Napp, D. T.; Bruckenstein, S. A Ring-Disk Electrode Study of the Current/Potential Behaviour of Platinum in 1.0 M Sulphuric and 0.1 M Perchloric Acids. *Electrochim. Acta* **1970**, *15* (9), 1493−1509.
(13) Ehelebe, K.; Knöppel, J.; Bierling, M.; Mayerhöfer, B.; Böhm, T.; Kulyk, N.; Thiele, S.; Mayrhofer, K. J. J.; Cherevko, S. Platinum Dissolution in Realistic Fuel Cell Catalyst Layers. *Angew. Chem., Int. Ed.* **2021**, *60* (16), 8882−8888.
(14) Topalov, A. A.; Katsounaros, I.; Auinger, M.; Cherevko, S.; Meier, J. C.; Klemm, S. O.; Mayrhofer, K. J. J. Dissolution of Platinum: Limits for the Deployment of Electrochemical Energy Conversion? *Angew. Chem., Int. Ed.* **2012**, *51* (50), 12613−12615.
(15) Sugawara, Y.; Okayasu, T.; Yadav, A. P.; Nishikata, A.; Tsuru, T. Dissolution Mechanism of Platinum in Sulfuric Acid Solution. *J. Electrochem. Soc.* **2012**, *159* (11), F779−F786.
(16) Lopes, P. P.; Strmcnik, D.; Tripkovic, D.; Connell, J. G.; Stamenkovic, V.; Markovic, N. M. Relationships between Atomic Level Surface Structure and Stability/Activity of Platinum Surface Atoms in Aqueous Environments. *ACS Catal.* **2016**, *6* (4), 2536−2544.
(17) Topalov, A. A.; Cherevko, S.; Zeradjanin, A. R.; Meier, J. C.; Katsounaros, I.; Mayrhofer, K. J. J. Towards a Comprehensive Understanding of Platinum Dissolution in Acidic Media. *Chem. Sci.* **2014**, *5* (2), 631−638.
(18) Topalov, A. A.; Zeradjanin, A. R.; Cherevko, S.; Mayrhofer, K. J. J. The Impact of Dissolved Reactive Gases on Platinum Dissolution in Acidic Media. *Electrochem. Commun.* **2014**, *40*, 49−53.
(19) Cherevko, S.; Zeradjanin, A. R.; Keeley, G. P.; Mayrhofer, K. J. J. A Comparative Study on Gold and Platinum Dissolution in Acidic and Alkaline Media. *J. Electrochem. Soc.* **2014**, *161* (12), H822−H830.
(20) Fuchs, T.; Drnec, J.; Calle-Vallejo, F.; Stubb, N.; Sandbeck, D. J. S.; Ruge, M.; Cherevko, S.; Harrington, D. A.; Magnussen, O. M. Structure Dependency of the Atomic-Scale Mechanisms of Platinum Electro-Oxidation and Dissolution. *Nat. Catal.* **2020**, *3* (9), 754−761.
(21) Cherevko, S.; Topalov, A. A.; Zeradjanin, A. R.; Keeley, G. P.; Mayrhofer, K. J. J. Temperature-Dependent Dissolution of Polycrystalline Platinum in Sulfuric Acid Electrolyte. *Electrocatalysis* **2014**, *5* (3), 235−240.
(22) Lopes, P. P.; Tripkovic, D.; Martins, P. F. B. D.; Strmcnik, D.; Ticianelli, E. A.; Stamenkovic, V. R.; Markovic, N. M. Dynamics of Electrochemical Pt Dissolution at Atomic and Molecular Levels. *J. Electroanal. Chem.* **2018**, *819*, 123−129.
(23) Wang, Z.; Tada, E.; Nishikata, A. *In-Situ* Monitoring of Platinum Dissolution under Potential Cycling by a Channel Flow Double Electrode. *J. Electrochem. Soc.* **2014**, *161* (4), F380−F385.
(24) Cherevko, S.; Kulyk, N.; Mayrhofer, K. J. J. Durability of Platinum-Based Fuel Cell Electrocatalysts: Dissolution of Bulk and Nanoscale Platinum. *Nano Energy* **2016**, *29*, 275−298.
(25) Myers, D. J.; Wang, X.; Smith, M. C.; More, K. L. Potentiostatic and Potential Cycling Dissolution of Polycrystalline Platinum and Platinum Nano-Particle Fuel Cell Catalysts. *J. Electrochem. Soc.* **2018**, *165* (6), F3178−F3190.
(26) Liang, D.; Shen, Q.; Hou, M.; Shao, Z.; Yi, B. Study of the Cell Reversal Process of Large Area Proton Exchange Membrane Fuel Cells under Fuel Starvation. *J. Power Sources* **2009**, *194* (2), 847−853.
(27) Bisello, A.; Colombo, E.; Baricci, A.; Rabissi, C.; Guetaz, L.; Gazdzicki, P.; Casalegno, A. Mitigated Start-Up of PEMFC in Real Automotive Conditions: Local Experimental Investigation and Development of a New Accelerated Stress Test Protocol. *J. Electrochem. Soc.* **2021**, *168* (5), 054501.
(28) Colombo, E.; Bisello, A.; Casalegno, A.; Baricci, A. Mitigating PEMFC Degradation during Start-Up: Locally Resolved Experimental Analysis and Transient Physical Modelling. *J. Electrochem. Soc.* **2021**, *168* (5), 054508.
(29) Kim, J.; Lee, J.; Tak, Y. Relationship between Carbon Corrosion and Positive Electrode Potential in a Proton-Exchange Membrane Fuel Cell during Start/Stop Operation. *J. Power Sources* **2009**, *192* (2), 674−678.
(30) Shen, Q.; Hou, M.; Liang, D.; Zhou, Z.; Li, X.; Shao, Z.; Yi, B. Study on the Processes of Start-Up and Shutdown in Proton Exchange Membrane Fuel Cells. *J. Power Sources* **2009**, *189* (2), 1114−1119.
(31) Taniguchi, A.; Akita, T.; Yasuda, K.; Miyazaki, Y. Analysis of Electrocatalyst Degradation in PEMFC Caused by Cell Reversal during Fuel Starvation. *J. Power Sources* **2004**, *130* (1), 42−49.
(32) Cooper, K. R.; Smith, M. Electrical Test Methods for On-Line Fuel Cell Ohmic Resistance Measurement. *J. Power Sources* **2006**, *160* (2), 1088−1095.
(33) Huang, X.; Wang, X.; Nergaard, T.; Lai, J.-S.; Xu, X.; Zhu, L. Parasitic Ringing and Design Issues of Digitally Controlled High Power Interleaved Boost Converters. *IEEE Trans. Power Electron.* **2004**, *19* (5), 1341−1352.
(34) Cherevko, S.; Keeley, G. P.; Geiger, S.; Zeradjanin, A. R.; Hodnik, N.; Kulyk, N.; Mayrhofer, K. J. J. Dissolution of Platinum in the Operational Range of Fuel Cells. *ChemElectroChem.* **2015**, *2* (10), 1471−1478.
(35) Inzelt, G.; Berkes, B.; Kriston, Á. Temperature Dependence of Two Types of Dissolution of Platinum in Acid Media. An Electrochemical Nanogravimetric Study. *Electrochim. Acta* **2010**, *55* (16), 4742−4749.
(36) Imai, H.; Izumi, K.; Matsumoto, M.; Kubo, Y.; Kato, K.; Imai, Y. *In Situ* and Real-Time Monitoring of Oxide Growth in a Few Monolayers at Surfaces of Platinum Nanoparticles in Aqueous Media. *J. Am. Chem. Soc.* **2009**, *131* (17), 6293−6300.
(37) Muller, A. W. J.; Maessen, F. J. M. J.; Davidson, C. L. The Corrosion Rates of Five Dental Ni-Cr-Mo Alloys Determined by

https://doi.org/10.1021/jacsau.2c00474
JACS Au 2023, 3, 105−112

Chemical Analysis of the Medium using ICP-AES, and by the Potentiostatic De-Aeration Method. *Corros. Sci.* **1990**, *30* (6), 583−601.
(38) Andreas, H. A. Self-Discharge in Electrochemical Capacitors: A Perspective Article. *J. Electrochem. Soc.* **2015**, *162* (5), A5047−A5053.
(39) Black, J.; Andreas, H. A. Effects of Charge Redistribution on Self-Discharge of Electrochemical Capacitors. *Electrochim. Acta* **2009**, *54* (13), 3568−3574.
(40) Harrington, D. A.; Conway, B. E. Kinetic Theory of the Open-Circuit Potential Decay Method for Evaluation of Behaviour of Adsorbed Intermediates: Analysis for the Case of the H_2 Evolution Reaction. *J. Electroanal. Chem.* **1987**, *221* (1), 1−21.
(41) Bard, A. J.; Faulkner, R. L. *Electrochemical Methods and Applications*, 2nd ed.; Wiley: New York, 2001.
(42) Newman, J. S.; Tobias, C. W. Theoretical Analysis of Current Distribution in Porous Electrodes. *J. Electrochem. Soc.* **1962**, *109* (12), 1183.
(43) Obut, S.; Alper, E. Numerical Assessment of Dependence of Polymer Electrolyte Membrane Fuel Cell Performance on Cathode Catalyst Layer Parameters. *J. Power Sources* **2011**, *196* (4), 1920−1931.
(44) Abedini, A.; Dabir, B.; Kalbasi, M. Experimental Verification for Simulation Study of Pt/CNT Nanostructured Cathode Catalyst Layer for PEM Fuel Cells. *Int. J. Hydrog. Energy* **2012**, *37* (10), 8439−8450.

https://doi.org/10.1021/jacsau.2c00474
JACS Au 2023, 3, 105−112